



Combined approach of a coupled fire model with atmospheric releases: the case of the 2003 Glacier wildfires

Germana Manca^{1*}, Guido Cervone² and Keith C. Clarke³

¹Environmental Science and Policy, 4400 University Dr., 22030 – GMU, Fairfax, Va

²Department of Geography, 302 Walker Building, 16802 – The Pennsylvania State University, University Park, Pa

³Department of Geography, 1832 Ellison Hall, 93106 – The University of Santa Barbara, Santa Barbara, Ca

*Corresponding author, e-mail address: gmanca@gmu.edu

Abstract

A combined GIS and remote sensing approach is applied to map and model the Glacier National Park wildfires of the summer 2003. Numerical simulations were performed using the Clarke Fire Automaton Model, and the fire extents were associated with the atmospheric plumes, observed using remote sensing data from the MODerate resolution Imaging Spectro-radiometer and Total Ozone Mapping Spectrometer. The wildfire simulation results show a correlation between the predicted and the actual fires. Remote sensing data are used to quantify the optical dimming of the atmosphere caused by the fires. The observed atmospheric dimming is correlated both spatially and temporally, with the fire simulations. Such knowledge is crucial to build a coupled land-atmosphere fire model.

Keywords: GIS, RS, Wildfire, atmospheric dimming, modelling.

Introduction

Fire spread models assess the rate at which a wildfire spreads over a surface, taking into account the chemical, physical, and geometrical characteristics of the fire terrain; and the temperature, humidity and wind characteristics of the atmosphere [Scott and Burgan, 2005; Siljander, 2009; Zhang et al., 2010]. They compute the chemical and physical fluxes, and use them to determine the fire spread over the geographical domain [Rothermel, 1972]. Anderson and Brown [1988] have defined approaches to model fire geometry in relation to wind speed and terrain slope. In their model the shape of the wildfire is prevalently elliptical, and the eccentricity and orientation of the semi-major axis of the ellipsis are determined by wind speed, direction, and terrain slope. Thus, in the absence of wind and on a flat surface, the elliptical shape becomes circular. More complex models have been developed, and the appropriateness of a model for a fire situation is determined by the model bias, complexity, available input data, environmental conditions, computational resources, ability to calculate parameters easily estimated by fire fighters, and time availability [Mandel et al., 2008].

Fire models vary from those that simply calculate the rate of spread over time, to complex computer simulation models that incorporate fire threat analysis. The latest model, Flam Map (based on the FARSITE model) computes the magnitude and the azimuth of the maximum spread rate, and the elliptical characteristics of the fire shape [Finney, 2006]. However, uncertainty in the input variables can have a substantial impact on the resulting propagation errors [Bachmann and Allgöwer, 2002]. In order to improve safety and effectiveness, there is a need for advanced warning for wildfire evacuation provided by dynamic GIS approaches [Pultar et al., 2008].

The Anderson model was based on several simplifying assumptions about wind direction, slope and aspect of topography, fuel load variations, and fire spread rates--each a critical component contributing to fire behavior. In reality, fires show irregular burn patterns and their behavior is shaped in unpredictable ways by the factors listed above, including unburned patches and outlying spot fires. As a result, the fire footprint appears chaotic. It is impossible to fully anticipate the interrelationships between the causal variables and the resulting behavior as fire appears to have both random and complex components, including non-linear feedbacks.

For example, once a fire starts it forms its own localized fire weather, further modifying behavior, similarly forward spot fires can burn fuel and actually stop the advance of a main front [Clarke and Olson, 1996]. Random processes and complexity can generate forms that are fractal in nature. In this case, a fractal process may better predict the behavior of a fire and the resulting shape of the fire scar or burned area. Accordingly, wildfires are considered complex phenomena due to the relationship of the variables which influence the fire behavior. Fire in an open uncontrolled environment is recognized as chaotic, and the chaotic process can be simulated through numerical modeling.

This study applies the Clarke Cellular Automaton Fire Model to simulate the large Glacier wildfires [Clarke et al., 1995]. This model was previously tested using data from California's Santa Cruz Mountains [Clarke and Olson 1996], and the behavior and spread of the 1998 summer wildfire in the area of Northern Sardinia, Italy [Manca, 1998].

The Clark Cellular Automata Fire Model approach shows a strong self-affinity with fractal theory, and perfectly matched the pattern of the wildfire and the above mentioned chaos theory, allowing outlying spot fires and unburned perforations in the fire scars.

Forest fires are known for increasing aerosols (contaminants) in the atmosphere, and these contaminants severely affect the Earth's environment [Bourcier et al., 2010]. Aerosol particles such as smoke, ash and soot can affect the climate system by reflecting, absorbing and scattering radiation. As a result, aerosols play a role in both the cooling and warming of the Earth. The study of atmospheric emissions is also crucial to identify high risk areas of contamination harmful to human health [Cervone et al., 2008]. Once injected in the atmosphere, the aerosol particles have varying resident times, which are affected by the size of the particles, and weather condition such as precipitation and wind patterns [Albriet et al., 2010]. It is very difficult to continuously observe aerosol distributions because they quickly mix and are transported and dispersed by the atmospheric circulation. However with the advent of remote sensing, it is now possible to quantify atmospheric aerosol concentrations, and to study their interaction with natural and man made phenomena like forest fires [Amraoui et al., 2010; Barrett et al., 2010].

One of the drawbacks of the proposed fire model is the inability to assess the atmospheric effects of the fire. It is generally very hard to compute the amount of aerosols released into the atmosphere from a fire, due to the many factors involved, such as the characteristics of the burning mass, the moisture content, temperature, wind characteristic, etc. With the

eventual goal of developing a joint land-atmosphere fire model as a first step, we have investigated the relationship between burned area and atmospheric dimming as detected by remote sensing instruments. Using data from the NASA Moderate Resolution Imaging Spectroradiometer (MODIS) and the Total Ozone Mapping Spectrometer (TOMS), we have computed spatio-temporal statistics of the atmospheric dimming associated with the fire. In this research, we used a combined approach using a GIS-based fire model and remote sensing data to simulate the progression of wildfires, and their atmospheric effects, that occurred in Glacier National Park during the summer of 2003 (Fig. 1 a,b,c). Several large fires occurred during mid July to mid September, burning about 125,400 hectares.

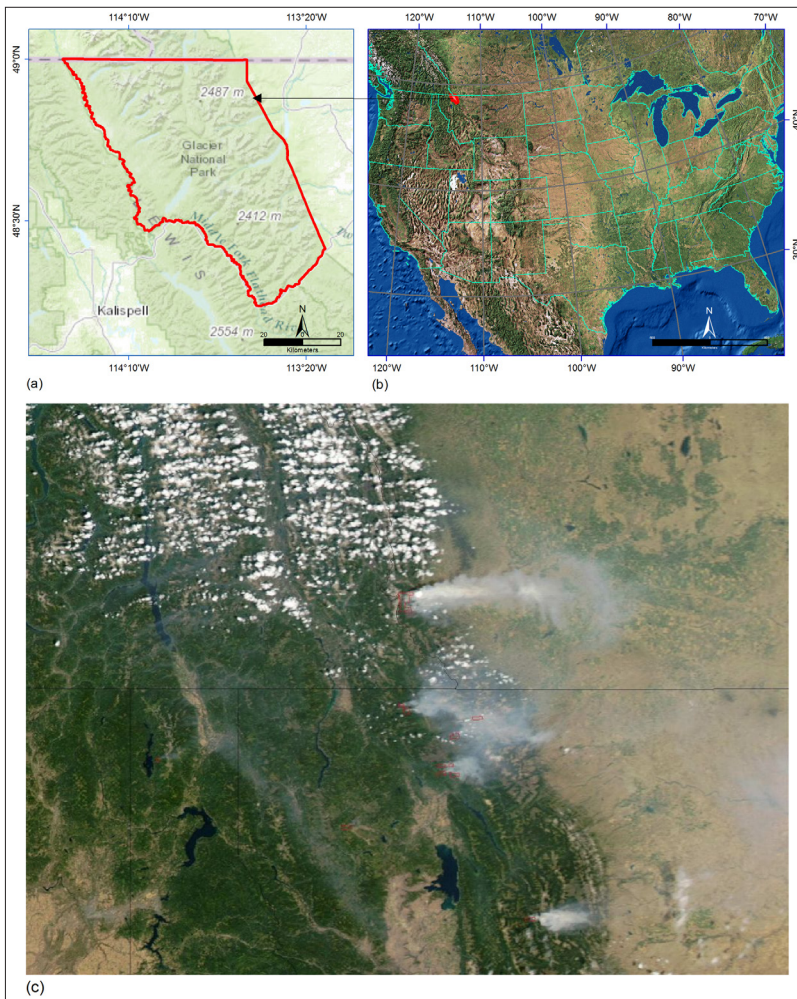


Figure 1 - Geographical location of the Glacier National Park (a,b) and park's forest fires (c) observed by MODIS. Sources Esri, DeLorme, NAVTEQ, TomTom, Intermap, increment P Corp., GEBCO, USGS, FAO, NPS, NRCAN, GeoBase, IGN, Kadaster NL, Ordnance Survey, Esri Japan, METI, Esri China (Hong Kong), swisstopo, and the GIS User Community.

MODIS is a moderate resolution multi-spectral sensor currently flying on two NASA satellites, AQUA and TERRA. MODIS measures emissivity over the visible to InfraRed spectrum. A description of the MODIS aerosols products and their comparison with in situ measurements is discussed by Chu et al. [2002]. While the AQUA satellite was designed to observe the Earth's water cycle, the TERRA satellite was designed to collect data relating to the Earth's biogeochemical and energy systems. This study is based on standard TERRA MODIS Level 3, 4.63 km gridded monthly composite products. The gridded data is generated by binning and averaging the nominal 1 km swath. Moreover MODIS data can be freely obtained through direct broadcast, which requires an X-band antenna and its control equipment, or from the NASA MODIS website.

The Total Ozone Mapping Spectrometer (TOMS) has been flying since the 1970s onboard a series of different spacecrafts, to measure different characteristics of the atmosphere, including the relative amount of aerosols. TOMS aerosol index is related to aerosol optical depth, and it is a unitless measurement of the optical properties of scattering and aerosols absorption. Very low values less than 0.5 indicate a minuscule amount of suspended particles, whereas values larger than 4 indicate a particulate amount effectively occluding visibility. Herman et al. [1997] showed the global distribution of aerosols using TOMS. Hsu et al. [1996] have shown how it is possible to use TOMS AI data to detect biomass burning from space.

GIS Fire Model

The Clarke model was initially developed to run on a particular Unix operating system, and has been ported to the Windows and Linux operating systems. These versions are now available to run the model, thereby allowing more widespread model use. The software architecture is flexible, modular, and scalable, and allows relatively simple implementation.

The model gathers and couples fire determinants, therefore during a wildfire event, the determinants are clarified in the Figure 2 below.

The data inputs for the model are raster images, while the atmospheric variables are alphanumeric values. One group of variables considered for the simulation is air temperature, relative humidity, wind magnitude and wind direction. Although air temperature, wind direction, and air humidity are parameters deductible from the weather information, wind magnitude must be accurate to explain the fire behavior. The wind magnitude is a parameter related to the wind table. More specifically, it is a matrix of probabilities of fire movement at different headings and wind magnitudes. The probabilities in the wind tables are derived from the ellipses of the Anderson geometry fire spread. When the wind has no magnitude, the fire shows a 12% chance of spreading in the eight Moore-neighborhood directions. As the wind increases in magnitude, from 0 to 7, directionality becomes more pronounced. Whenever a firelet starts from a point of ignition, it moves across a surface, which is the weighted result of combining several geographic layers. The first input of the ignition is given by the weighted wind magnitude and direction. The other group of variables represents the geographic context. These variables have been computed and extracted from the geographic layers. This process includes conversion of a vector file to a raster file, in portable network graphics raster format, (png), transferring common coordinates, and numbers of rows and columns. At the end of the simulation, the resulting images are overlain with the original coverage to visualize the modeled process. Raster input variables for the fire consist of a fuel load image, soil moisture image, topography image in the form of a DEM, roads images, and an hillshade image for backdrop purposes. A brief description is provided below.

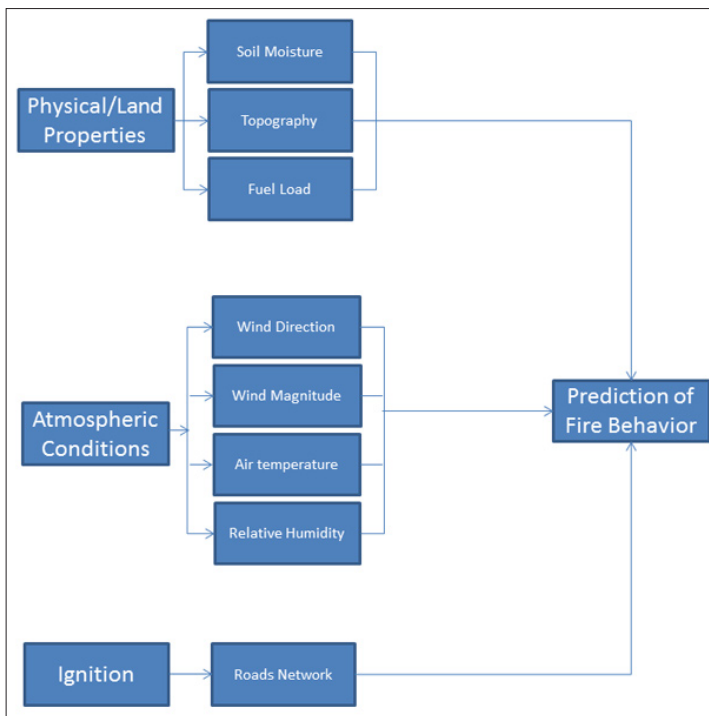


Figure 2 - Fire Determinants.

Fuel Load: is the dry weight of fuel per unit area. Loading or mass per unit area is usually expressed in metric tons/hectare. In this application the fuel loading is expressed in megagrams/pixel. The ignition, buildup, and behavior of the fire mainly depend on the availability and condition of the fuel. The combustible material is the basis for an estimation of a potential mass that is burned by a fire. A vegetation map was downloaded from the Glacier National Park web site. This map derived from the stereo interpretation of August 1999 true color aerial photograph, which the polygon units were mapped to 0.5 ha (1.25 acres) (<http://www1.usgs.gov/vip/glac/metaglacspatial.xml>). The vegetation has been translated into fuels loading map. Surface fuel includes loose surface litter on the forest floor, grasses, and any low shrubs. The fuel loading is made up of different types of plants [Kelty et al., 2008]. Due to the lack of information on fire fuel parameters, specifically for some types of vegetation, it has been assumed that the dominant species classes cover an entire pixel. Most of the trees were grouped into major classes. A subsequent calculation of the total biomass was divided among the number of pixels belonging to the patch for that particular vegetation type.

Soil Moisture: Landsat ETM images of July/August 2003 have been downloaded from the USGS website. Images are fused together to compensate for missing values. The background noise was removed from the histogram of the resulting image. The spatial and radiometric resolution has been preserved, and a fusion of the multispectral bands and PAN has been carried out. The algorithm, created by the 5/7 band ratio in red, emphasizes the soil moisture. Obviously the moisture level is higher close to the perennial glacier, and taking

down toward the valley. Due to the dry weather of the summer 2003, caused by a five year drought and a summer season of almost no precipitation, the soil moisture level is lower than the average [Climate Prediction Center, Soil Moisture, 2003].

Topography: was derived from the digital elevation model, from the Glacier web site (Glacier National Park 30 meter Digital Elevation Model. Glacier National Park GIS Program). The DEM has been used to calculate the slope in each grid cell. As discussed previously, the topography of a region has a significant role in determining fire behavior. This is further enhanced by the fact that the elevation characteristics of the study area vary greatly.

Roads: most ignition points start close to the road network because other than lightening, arson is the leading cause of wildfire ignition. Therefore, a 100m buffer of the network system was provided. If the starting point of the wildfire is not provided, a random firelet is supposed to start within this buffer. In this case the firelet is localized at the supposing starting point of the wildfire.

Hillshaded image: is used as a backdrop for the simulation and to sketch the surface texture. It has been created, using 315° as azimuth angle of the light source, 45° as altitude angle of the light source at the horizon.

The fire behavior determinant characteristics are explicated in the fire model used in this application, where the fire spread is a process that closely resembles Diffusion Limited Aggregation (DLA, which is a process oriented model, assuming that an object will grow and change shape due to a large number of essentially random events, each of which is influenced by the events that preceded it. In the context of fires, DLA can be thought of as a process by which “firelets” are sent out one at a time from one or more fire sources. The process has been implemented as a cellular automaton. The cellular automata modeling paradigm and its extension within the framework of Geo-Algebra are extensively described by Takeyama and Couclelis [IJGS, 1997]; the described application is registered to the cells of a regular grid, which coincides with the resolution of the Digital Elevation Model (DEM). Ignition consists of a single moving firelet. If the firelet finds fuel, it ignites the fuel and moves in a direction determined by the local fire environment. If there is no fuel at its new location, or if the firelet has moved too far from its source, the firelet stops. The next firelet then moves out from the fire center. If this firelet finds a cell that has already been burned, the firelet continues on its journey to find fuel. Upon finding unburned fuel, the firelet ignites it and stops. The cellular automata model uses the mentioned and stored set of GIS data (DEM, fuel loading, road network, and fuel moisture), and fire atmospheric variables (air temperature, wind magnitude and direction, relative humidity). After inputting these data, the program simulates fire ignition at a location given by the user so that any number of simulated fires can be started simultaneously or at set times and places. The Monte Carlo version of the model allows the user to repeat one or more simulated fires under similar or differing conditions many times, in each case accumulating the likelihood that a pixel is burned. It is also used to compute probability estimates and the model can do so either for constant or variable fire environment conditions.

Glacier National Park

Glacier National Park (Fig. 1a) is located in Northern Montana, USA, covering an area of 405,000 hectares of forests, alpine meadows, and lakes. The park is adjacent to the Canadian Waterton Lakes National Park, and together they form the Waterton-Glacier

International Peace Park. Glacier National Park is affected by an average of 15 fires each summer and has averaged 2000 hectares burned each year. Most fires are short in length, lasting less than two weeks. During the summer of 2003, Glacier National Park was affected by several large fires during mid-July to mid-September, which destroyed about 125,400 hectares. Such fires could be observed using spaceborne observations (<http://www.nasa.gov/centers/goddard/news/topstory/2003/0729glacier.html>) using the MODIS onboard the TERRA satellite.

Results

The parameters used to run the model included the following weather conditions: 7 wind direction (come from the north); 6 wind magnitude (scale from 1 to 7); 30 air temperature (degree Celsius); 20% relative humidity. A fire is ignited at a location given by the user. A random number is then drawn to determine direction of movement. The new firelet location is then burned, and the fires move on. Each fire center continues to generate random fire “runs” of a length that reflects the fuel moisture and pre-heating conditions until its firelets find no unburned fuel. When successive runs find no new fuel to burn, this fire center goes out. The burned area is a place of 1.127 million tons of biomass. In the area considered, where the wildfire was most dangerous, the amount of burnt surface in the simulation was 98.87 square kilometers, whereas, the actual fire burned 124.68 square kilometers. The rounded ratio between the real and the simulated fire extent is 80%, a 20% underestimate. Figure 3 shows the simulated and observed burned area.

A first approach to identify the comparison between the two images has been carried out through a statistic analysis. The results of this analysis are highlighted in the Table 1.

Table 1 - Correlation matrix. Statistics of individual layers.

Layer	Real	Simulation
Real	1.00000	0.66603
Simulation	0.66603	1.00000

The correlation matrix reports a value of high positive linear correlation. In this case the variable pair shows a concordance between the two geographic layers. Further analysis is necessary to accurately determine the behavior of the two geographic layers. The approach is based on a map comparison. This is performed by a crosstabulation matrix, where the rows are classes of the comparison map and the columns are classes of the reference map. The analysis, applied to verify the correspondence of the two maps, is based on the composite operator, in which the assessment of the agreement is calculated through a diagonal entries and off-diagonal entries [Pontius and Cheuk, 2006; Pontius and Kuzera, 2008; Pontius and Connors, 2009], applying soft-classification. The location of the pixel, inside the boundaries of the pixel, determines the magnitude of agreement, if its position is on the diagonal, or disagreement, if it is outside. The crosstabulation matrix at the fine resolution reports the same results for the minimum, multiplication, and composite rules, and the overall agreement is 84, 07%. Moving forward to the medium resolution the agreement still grows, at a low percentage, to reach 84, 15% at the coarsest resolution. This behavior is justified by the meaning of the composite operator. It refers to the agreement within the boundaries of a pixel; consequently larger boundaries mean larger agreement. This result

outlines the high correlation between the two matrices, and the overall agreement between the maps remains the same.

Although there is a very high degree of correspondence between the observed satellite data and the simulation results, there are both false positives (burned areas in the simulation but not in the observed data) and false negatives (burned areas in the observed data, but not in the simulation).

In order to study the atmospheric dimming associated with this large volume of biomass burning, an in depth analysis of the atmosphere's optical properties was performed using the NASA TOMS and MODIS. Aerosol Optical Depth (AOD) data from MODIS (TERRA) level 3 atmospheric monthly product, generated by combining the daily mean of AOD at 0.55 microns for both ocean and land. The analysis is based on 46 months of data from March 2000 to December 2003 which were downloaded from the NASA EOS Gateway. The data covers the region bounded by latitude 42N to 52N and longitude 103W to 120W, with resolution of 1o latitude and 1o longitude. MODIS data, available on a monthly basis, was paired with Aerosol Index (AI) data from the TOMS (EarthProbe) daily product.

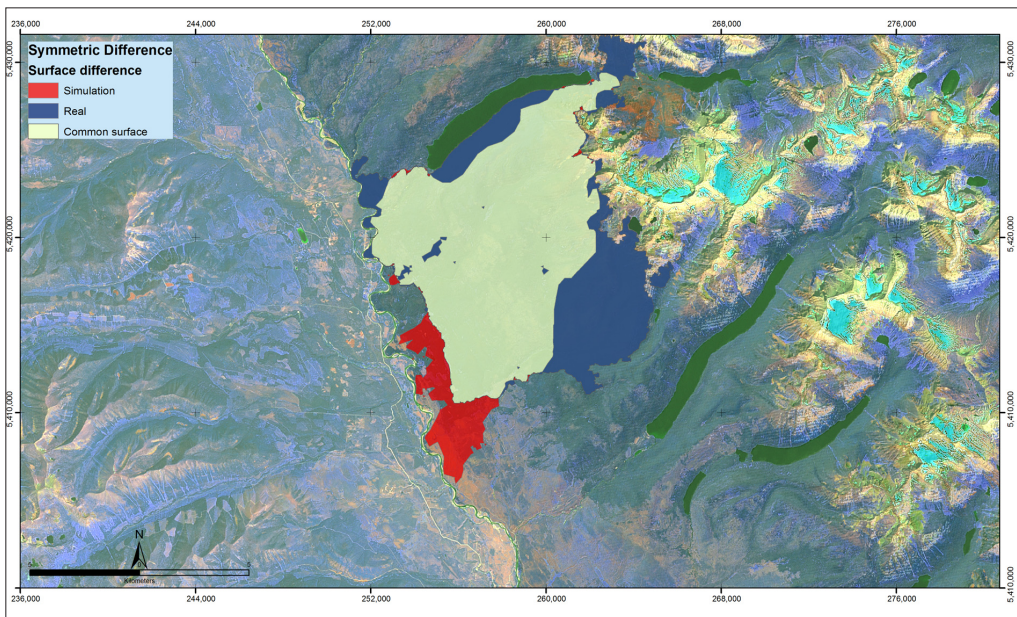


Figure 3 - Comparison between simulated and observed burned area. Red area indicates false positive, while the blue area, false negative. The beige area is the correct estimation by the model.

Figure 4 shows the sequence of AOD from July 2003 to October 2003. These four show the AOD time series for six different locations of the Glacier National Park. In all graphs a strong seasonal effect is present, showing AOD oscillations from 0.5 during the winter months to 0.4 during the summer months. The AOD is notably high in July, August and September, reaching maximum values in August.

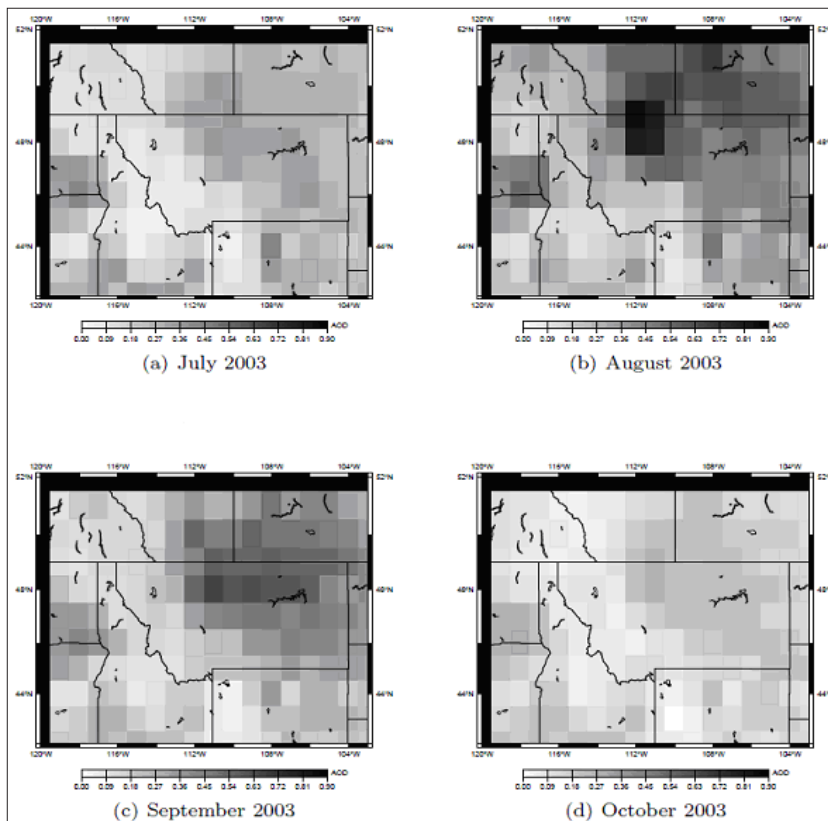


Figure 4 - Aerosol Optical Depth for Summer 2003.

In all graphs, a single prominent AOD peak of 0.9 is found in August 2003, corresponding to the time and place of the forest fires. The high monthly data values are due to the prolonged burning of forest which occurred in this region, leading to a large increase of the AOD. The lower mean values of July and September with respect to August are due to the presence of forest burning only in half of the months, because the largest fires were detected at the end of August.

Figure 5 shows the AI time series for six locations of the Glacier National Park. The locations for the time-series closely correspond to the locations in Figure 4. Figure 6 shows the AI time-series for year 2003, its 30-day average computed using data from 2000 to 2002 (3 years), and 1 and 2 standard deviation (σ). The graphs correspond to the locations of Figure 4. There are prominent peaks, in all of the graphs, (as high as 5 σ), during the months of July, August and September, due to these forest fires, consistent with increases in MODIS AOD measurements. Values, as high as 37, are recorded towards the end of August 2003. Such a prominent increase is due to the large amount of biomass burning.

Therefore the amount of atmospheric dimming caused by the fires corresponds to a 100% increase from .04 to .08 in AOD data. With respect to AI data, the maximum daily variation shows an increase of about 5 σ , with a peak of 37.

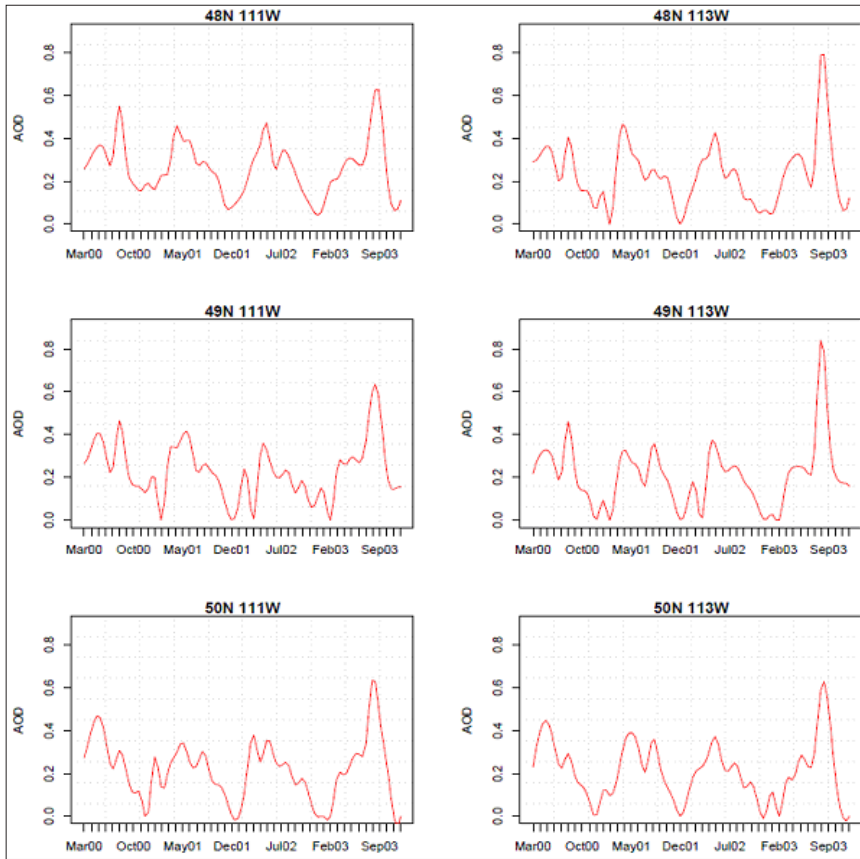


Figure 5 - Time Series for several locations over the Glacier National Park using MODIS data.

Conclusion

This paper presented an integrated approach of the Clarke Automaton Fire model to the large 2003 forest fires of the Glacier national park and the analysis of the atmospheric dimming retrieved from NASA satellite data. The results are the first step into developing a land-atmosphere coupled fire model.

The fire model simulations were validated with land cover observations. A GIS approach was employed to compute the error between in the estimation of the burned area. A comparison of the observed and simulated burned area maps show a correlation of over 80% between the real and simulated data

Due to the model's inability to estimate the generation of atmospheric particulates, we have analyzed the optical atmospheric dimming associated with the fires using data from MODIS and TOMS instruments. The large atmospheric dimming observed both spatially and temporally is associated with the biomass burning. In particular, we have observed a 100% increase in AOD values, and 500% increase in AI values.

These results are encouraging in our goal of building an integrated fire-atmosphere coupled model.

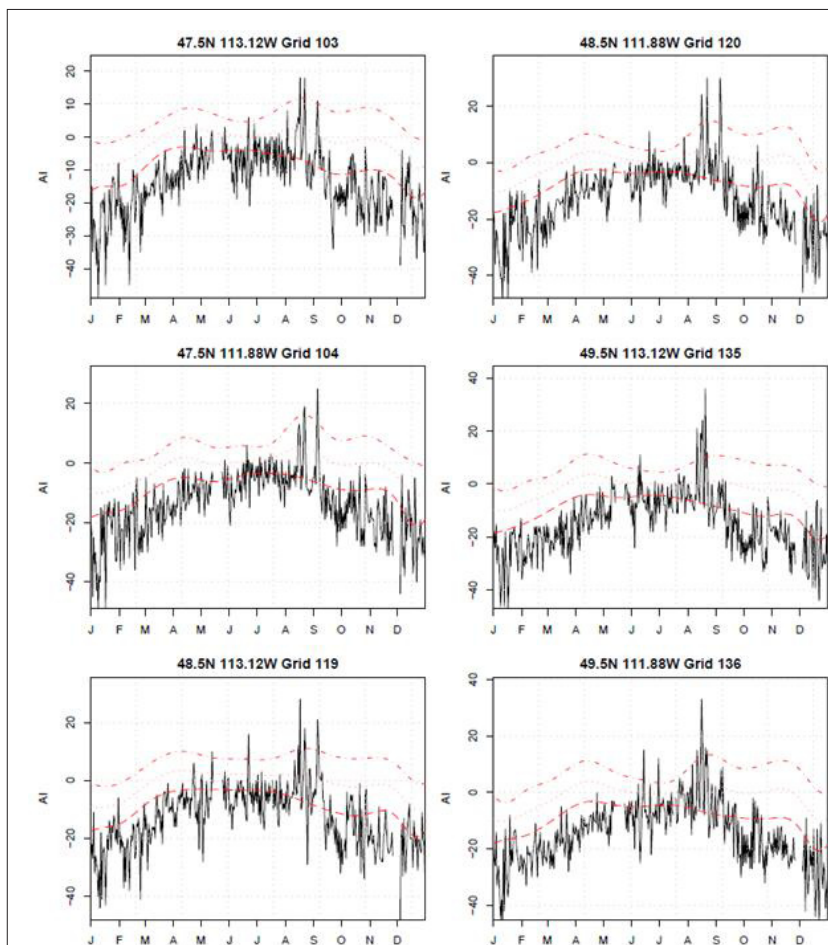


Figure 6 - AI time-series from TOMS for different locations.

Acknowledgements

Initial results relative to this work were presented at the 2012 IGARSS Geoscience and Remote Sensing Society

References

- Albriet B., Sartelet K., Lacour S., Carissimo B., Seigneur C. (2010) - *Modelling aerosol number distributions from a vehicle exhaust with an aerosol cfd modelⁿ*. Atmospheric Environment, 44 (8): 1126-1137. doi: <http://dx.doi.org/10.1016/j.atmosenv.2009.11.025>.
- Amraoui M., Da Camara C., Pereira J. (2010) - *Detection and monitoring of african vegetation fires using msg-seviri imagery*. Remote Sensing of Environment, 114 (5): 1038-1052. doi: <http://dx.doi.org/10.1016/j.rse.2009.12.019>.
- Anderson H. E., Brown J. K. (1988) - *Fuel characteristics and fire behavior considerations in the wildlands*. In: Protecting people and homes from wildfire in the interior west: proceedings of the symposium and workshop. USDA Forest Service, General Technical

- Report INT-251. Intermountain Research Station. Ogden, UT. pp. 124-130.
- Bachmann A., Allgöwer B. (2002) - *Uncertainty propagation in wildland fire behavior modeling*. International Journal of Geographical Information Science, 16 (2): 115-127. doi: <http://dx.doi.org/10.1080/13658810110099080>.
- Barrett K., Kasischke E., McGuire A., Turetsky M., Kane E. (2010) - *Modeling fire severity in black spruce stands in the alaskan boreal forest using spectral and non-spectral geospatial data*. Remote Sensing of Environment, 114 (7): 1494-1503. doi: <http://dx.doi.org/10.1016/j.rse.2010.02.001>.
- Bourcier L., Sellegrì K., Masson O., Zangrando R., Barbante C., Gambaro A., Pichon J.-M., Boulon J., Laj P. (2010) - *Experimental evidence of biomass burning as a source of atmospheric ¹³⁷Cs, puy de Dôme (1465 m a.s.l.), France*. Atmospheric Environment, 44 (19): 2280-2286. doi: <http://dx.doi.org/10.1016/j.atmosenv.2010.04.017>.
- Cervone G., Franzese P., Ezber Y., Boybeyi Z. (2008) - *Risk assessment of atmospheric emissions using machine learning*. Natural Hazards and Earth System Science, 8: 991-1000. doi: <http://dx.doi.org/10.5194/nhess-8-991-2008>.
- Chu D.A., Kaufman Y.J., Ichoku C., Remer L.A., Tanré D., Holben B.N. (2002) - *Validation of MODIS aerosol optical depth retrieval over land*. Geophysical Research Letters, 29 (12): MOD2,1-4. doi: <http://dx.doi.org/10.1029/2001GL013205>.
- Clarke K.C., Olson G. (1996) - *Refining a cellular automaton model of wildfire propagation and extinction*. GIS and Environmental Modeling: Progress and Research Issues, GIS world books Edition, pp. 333-338.
- Clarke K.C., Riggan P., Brass J.A. (1995) - *A cellular automaton model of wildfire propagation and extinction*. Photogrammetric Engineering and Remote Sensing, 60 (11): 1355-1367.
- Devineau J.L., Fournier A., Nignan S. (2010) - *Savanna fire regimes assessment with MODIS fire data: Their relationship to land cover and plant species distribution in western Burkina Faso (West Africa)*. Journal of Arid Environments, 74 (9): 1092-1101. doi: <http://dx.doi.org/10.1016/j.jaridenv.2010.03.009>.
- Finney M.A. (2006) - *An overview of FlamMap fire modeling capabilities*. In: Andrews, P.L., Butler, B.W. (comps), Fuels Management-How to Measure Success: Conference Proceedings. Portland, OR, March 28-30, 2006, pp. 213-220; Proceedings RMRS-P-41, USDA Forest Service, Rocky Mountain Research Station, Fort Collins, CO.
- Kelty M.J., D'Amato A.W., Barten P.K. (2008) - *Silvicultural and Ecological considerations of Forest Biomass Harvesting in Massachusetts*. In Massachusetts Department of Natural Resources Conservation, University of Massachusetts Amherst, MA.
- Herman J.R., Bhartia P.K., Torres O., Hsu C., Seftor C., Celarier E. (1997) - *Global distribution of UV-absorbing aerosols from Nimbus 7/TOMS data*. Journal of geophysical research, 102 (D14): 16911-16922. doi: <http://dx.doi.org/10.1029/96JD03680>.
- Hsu N.C., Herman J.R., Bhartia P.K., Seftor C.J., Torres O., Thompson A.M., Holben B.N. (1996) - *Detection of biomass burning smoke from TOMS measurements*. Geophysical Research Letters, 23 (7): 745-748. doi: <http://dx.doi.org/10.1029/96GL00455>.
- Manca G. (1998) - *The use of GIS and computational modeling with an application to forest fire management: a case study of Northern Sardinia*. ESRI 13th European Conference, Firenze, Italy.
- Mandel J., Bennethum L.S., Beezley D.J., Coen L.J., Douglas C.C., Kim M., Vodacek A. (2008) - *A wildland fire model with data assimilation*. Mathematics and Computers in

- Simulation, 79 (3): 584-606. doi: <http://dx.doi.org/10.1016/j.matcom.2008.03.015>.
- Rothermel R. (1972) - *A mathematical model for predicting fire spread in wildland fuels*. Technical Report RP-INT-115, U.S. Department of Agriculture, Intermountain Forest and Range Experiment Station.
- Scott J., Burgan R., (2005) - *Standard fire behavior fuel models: a comprehensive set for use with Rothermel's surface fire spread model*. Technical Report. RMRS-GTR-153, U.S. Department of Agriculture, Forest Service, Rocky Mountain Research Station.
- Siljander M. (2009) - *Predictive fire occurrence modeling to improve burned area estimation at a regional scale: A case study in east Caprivi, Namibia*. International Journal of Applied Earth Observation and Geoinformation, 11 (6): 380-393. doi: <http://dx.doi.org/10.1016/j.jag.2009.06.004>.
- Pontius R.G., Cheuk M.L. (2006) - *A generalized cross-tabulation matrix to compare soft-classified maps at multiple resolutions*. International Journal of Geographical Information Science, 20 (1): 1-30. doi: <http://dx.doi.org/10.1080/13658810500391024>.
- Pontius R.G., Kuzera K. (2008) - *Importance of matrix construction for multiple-resolution categorical map comparison*. GIScience & Remote Sensing, 45 (3): 249-274. doi: <http://dx.doi.org/10.2747/1548-1603.45.3.249>.
- Pontius R.G., Connors J. (2009) - *Range of categorical associations for comparison of maps with mixed pixels*. Photogrammetric Engineering & Remote Sensing 75 (8): 963-969. doi: <http://dx.doi.org/10.14358/PERS.75.8.963>.
- Pultar E., Raubal M., Cova T.J, Goodchild M.F. (2009) - *Dynamic GIS case studies: Wildfire evacuation and volunteered geographic information*. Transactions in GIS 13 (s1): 85-104. doi: <http://dx.doi.org/10.1111/j.1467-9671.2009.01157.x>.
- Takeyama M., Couclelis H. (1997) - *Map dynamics: integrating cellular automata and GIS through GeoAlgebra*. International Journal of Geographical Information Science, 2 (1): 73-91. doi: <http://dx.doi.org/10.1080/136588197242509>.
- Zhang Z., Zhang H., Zhou D. (2010) - *Using gis spatial analysis and logistic regression to predict the probabilities of human-caused grassland fires*. Journal of Arid Environments 74 (3): 386-393. doi: <http://dx.doi.org/10.1016/j.jaridenv.2009.09.024>.